

Global warming profoundly changes the spatial distribution of nitrogen use and losses in croplands

Chenchen Ren

Zhejiang University

Xiuming Zhang

The University of Melbourne <https://orcid.org/0000-0002-1961-3339>

Stefan Reis

UK Centre for Ecology & Hydrology <https://orcid.org/0000-0003-2428-8320>

Jiixin Jin

Hohai University

Jianming Xu

Zhejiang University <https://orcid.org/0000-0002-2954-9764>

Baojing Gu (✉ bjgu@zju.edu.cn)


Zhejiang University <https://orcid.org/0000-0003-3986-3519>

Article

Keywords:

Posted Date: July 5th, 2022

DOI: <https://doi.org/10.21203/rs.3.rs-1715654/v1>

License:  This work is licensed under a Creative Commons Attribution 4.0 International License. [Read Full License](#)

Version of Record: A version of this preprint was published at Nature Food on April 13th, 2023. See the published version at <https://doi.org/10.1038/s43016-023-00730-z>.

Abstract

Maintaining food production while reducing agricultural nitrogen pollution is a grand challenge under the threats of global climate change, which has exerted negative impacts on agricultural sustainability. How global agricultural nitrogen use and loss respond to climate change on temporal and spatial scale is rarely understood. Here we show that climate change leads to small temporal but substantial spatial changes in cropland nitrogen use and losses across global regions based on historical data for the period 1961-2018 from 150 countries. Increases of yield, nitrogen surplus and nitrogen use efficiency (NUE) are identified in 24% of countries, while reductions are observed for the remaining 76% of countries, as a result of climate change in 2018. Changes of cropland area per capita of rural population (CAPRP) further intensify the variations of nitrogen use and pollution in global croplands. Yet, improving farmers' practices with changes of CAPRP can facilitate climate change adaptation, by which global cropland NUE could be increased by one-third in 2100 compared to 2018 under future shared socioeconomic pathways. Our results would be of great significance to sustain global agriculture as well as eliminate national inequalities on food production and agricultural pollution control.

Full Text

Global climate change has led to an increase in both average ambient temperatures observed and the frequency of extreme weather events, including dry-hot and precipitation extremes¹⁻³. These changes not only threaten human and ecosystem health, but also adversely affect agricultural production^{4,5}. Mitigating the negative impacts of climate change on agriculture is a grand challenge, in the context of safeguarding food security for a growing and increasingly wealthy global population.

Nitrogen (N) fertilizer use has fed about half of the global population⁶; however, only N use in croplands has exceeded the safe planetary boundary, leading to substantial environmental problems such as air and water pollution, biodiversity loss, soil acidification and climate change (ozone layer depletion and nitrous oxide (N₂O) emission)^{7,8}. Currently, over 100 million tonnes of fertilizer N is applied to global croplands annually and over half of the N is lost to the environment, leading to an average N use efficiency (NUE) below 50%, a critical indicator for agricultural sustainability^{8,9}. So far, climate change impacts have been rarely considered when developing management strategies for sustainable agricultural N use, as the focus has been primarily on the climate effects of N fertilizer use, such as N₂O emissions¹⁰. Yet, climate change can affect agricultural N use and losses, for instance, and warming temperatures can increase ammonia emissions from croplands^{11,12}. The warming climate has been shown to aggravate N pollution in Australia¹³. Eutrophication will become more prevalent during the 21st century due to precipitation pattern changes¹⁴.

Here, we quantified the impact of climate change (annual mean temperature, annual total precipitation and their quadratic terms) on global crop yield (in terms of N harvested including all crop species), fertilization (total N fertilizer use on croplands), NUE (N harvested by crop divided by total N input) and N surplus (N not harvested by crop) from temporal and spatial perspectives based on the long-term panel data for the period 1961-2018 from 150 countries. We combined data on all crops due to the effect of interaction of a variation of crops during rotations on NUE. Meanwhile, we used national data for the analysis, since policy regulations are normally determined at national scale with regard to food security objectives and agri-environmental aspects

and country borders exerts significant impact on N pollution ¹⁵, and gridded or subnational data on cropland N use and loss are unavailable for the period 1961-2018 in all the 150 countries. To understand the interaction between climate change and farmers' practices on N use and loss, cropland area per capita of rural population (CAPRP) is introduced. CAPRP can be used to depict changes in farmers' practices and management, as its significant correlation with farm size that is normally used to refer the technical level of farmers' practices (Table S1 and see Method for more details). Large-scale farming facilitated by increase of CAPRP typically indicates a different management scheme compared to smallholder farming, with improved knowledge, mechanization and farming facilities ¹⁶. A fixed effect panel model that can effectively eliminate the bias within time and country is used for the analysis of past-counterfactual scenarios (1961-2018) and predicting future trends (towards the year 2100) based on future Shared Socioeconomic Pathways (SSP) scenarios (more details see Methods).

Results And Discussion

Temporal and spatial variability under climate change

The average air temperature increased across regions worldwide from 1961 to 2018 (Fig. 1 and S1), varying from 0.36 °C (Latin America) to 2.28 °C (Former Soviet Union). The average air temperature in the high (60°-90° N) and middle latitudes (30°-60° N) of the Northern Hemisphere (HMNH) is generally lower than that in the remaining regions. However, the temperature increase is more significant in these colder regions, especially in North America and the Former Soviet Union. These variations in averages and changes lead to variability in N use and loss between croplands in different world regions.

Over the period from 1961 to 2018, global NUE declines on average by of 0.4% annually due to a rise in ambient temperature compared to a situation without global warming (Fig. 2g), with large spatial variations between colder countries in the HMNH and warmer countries in low latitudes (0°-30°) and the Southern Hemisphere (LSH) (Fig. 3g). Taking 2018 as an example, we compared the spatial impact of temperature increase on NUE changes by modeling historic counterfactual scenarios (see methods for details). Other confounding factors, such as economic development stage, technological advancement and crop types are controlled in the fixed effect panel model (Tables 1, S2 and S6). NUE increases were noted for about 27% of countries worldwide with an average value of 4% (1–13%) in a 2018 due to increasing temperatures, mainly in colder countries in the HMNH. For the remaining 73% of countries with a warmer climate in the LSH, rising temperatures have reduced NUE by an average of 6% (0–14%).

Table 1
Regression results of yield, fertilization and NUE under climate change

	Ln Yield		Ln Fertilization		Ln NUE	
	Model 1	Model 2	Model 3	Model 4	Model 5	Model 6
Temperature	2.54**	3.15**	-10.34*	-17.80***	3.62**	5.55***
	(1.109)	(1.410)	(6.007)	(5.553)	(1.579)	(1.872)
Temperature ²	-13.62***	-14.15***	21.24	43.40**	-17.80***	-22.30***
	(4.016)	(4.751)	(18.857)	(18.110)	(5.133)	(5.455)
Precipitation	2.78***	3.73***	-0.66	-1.96	2.65***	3.73***
	(0.573)	(0.667)	(1.337)	(2.145)	(0.777)	(0.801)
Precipitation ²	-5.30***	-9.44***	1.30	4.71	-5.15***	-10.42***
	(1.315)	(1.652)	(2.875)	(5.679)	(1.936)	(2.266)
Ln CAPRP (ha)	0.03	-0.05	-0.31**	-0.94**	0.11**	0.19
	(0.036)	(0.116)	(0.140)	(0.428)	(0.047)	(0.162)
Ln Fertilization	0.08***	0.08***			-0.14***	-0.14***
	(0.012)	(0.012)			(0.019)	(0.019)
Temperature × Ln CAPRP		-0.35		8.61**		-2.01
		(1.113)		(3.907)		(1.589)
Temperature ² × Ln CAPRP		2.66		-21.36*		6.49
		(2.989)		(11.338)		(4.671)
Precipitation × Ln CAPRP		0.91*		-2.34		1.05
		(0.538)		(1.981)		(0.724)
Precipitation ² × Ln CAPRP		-3.72***		5.04		-4.73***
		(1.317)		(4.479)		(1.663)
N	7076	7076	7130	7130	7076	7076

Each column represents a separate regression model. Stars indicate statistical significance: * $p \leq 0.1$, ** $p \leq 0.05$, *** $p \leq 0.01$. Standard errors are displayed in parentheses and are clustered at the country-level. Temperature and precipitation are the average temperature (10^2 °C) and total precipitation (10^4 mm) across the year, respectively. Yield is all crop harvest nitrogen (kg ha^{-1}). Fertilization refers to nitrogen fertilization input (kg ha^{-1}). NUE is an abbreviation of nitrogen use efficiency of the agricultural cropland system. Cash crop ratio, crop type, and irrigation have been controlled in all regression equations. All models include country and year fixed effects.

	Ln Yield		Ln Fertilization		Ln NUE	
Adjust R ²	0.93	0.93	0.87	0.87	0.84	0.84
Within R ²	0.21	0.22	0.04	0.05	0.27	0.28

Each column represents a separate regression model. Stars indicate statistical significance: * $p \leq 0.1$, ** $p \leq 0.05$, *** $p \leq 0.01$. Standard errors are displayed in parentheses and are clustered at the country-level. Temperature and precipitation are the average temperature (10^2 °C) and total precipitation (10^4 mm) across the year, respectively. Yield is all crop harvest nitrogen (kg ha^{-1}). Fertilization refers to nitrogen fertilization input (kg ha^{-1}). NUE is an abbreviation of nitrogen use efficiency of the agricultural cropland system. Cash crop ratio, crop type, and irrigation have been controlled in all regression equations. All models include country and year fixed effects.

Warming contributes to the NUE increase in the HMNH as a result of yield increases, while at the same time reducing fertilization, as observed for Canada and Russia. We noted an increase of 0–6% (0–5 kg N per ha) in yield in 12% of countries worldwide due to warming climate in 2018 (Fig. 3a, Extended Data Fig. 1), all of which are located in the HMNH. Meanwhile, the N fertilization rate declined in most of countries due to temperature increase due to the concurrent drought (except for countries in low latitudes)³, with an average of 7% (0–28%, 0–68 kg N per ha) (Fig. 3d, Extended Data Fig. 1). In contrast, NUE was reduced in the remaining 73% of warmer countries. One of the most important reasons is that most of these countries have a much larger proportion of yield loss even with the reduced fertilization, such as in Australia. Crop yield declined in Australia by about 5% (2 kg N per ha) (Fig. 3a). However, the N fertilization rate reduced by only about 2% (1 kg per ha).

Global N surplus has increased in the early part of the period, but decreased subsequently in line with temperature changes despite yield and NUE reductions (Fig. 2a, g, j). This suggests a reduction in excess N application since 1980s. This is mainly due to the comparatively larger reduction in fertilization versus global yield decline (Fig. 2a and 2d). Spatially, N surplus declined by 6% (0–34%, 0–91 kg per ha) in 32% of countries worldwide in 2018 compared to a situation without global warming, with hot spots distributed in the HMNH (Fig. 3j, Extended Data Fig. 1). In comparison, N surplus increased by 3% (0–24%, 0–184 kg per ha) in the remaining 68% of countries, mainly distributed in the LSH. For instance, in Canada and Russia, the N surplus has been reduced by more than 30% (12 kg per ha) in 2018. But at the same time, N surplus increased in Brazil and Central Africa at an average of 15% (9 kg per ha).

Generally, warming temperature causes minor temporal but considerable spatial variations in cropland N use and losses in different global regions. Countries in the HMNH benefit from temperature increase, irrespective of NUE and yield improvements or fertilizer and N surplus reduction. However, they are only a small number of global countries. Most of global countries in the LSH suffered negative impacts from warming climate. These different responses to climate change lead to national inequalities on agricultural N use that further cascades to the variability of food production and environmental quality. Additionally, changes in crop yield, fertilization, NUE and surplus have been minor when including a consideration of precipitation change over the same period, especially for N fertilization (Fig. 2). In 2018, changes in precipitation only are associated with approximately 0.5%, 0.05%, 0.4%, and 0.7% changes in global yield, fertilization, NUE and surplus, respectively (Fig. 3). The large spatial variability of precipitation within a country or region, such as in China and USA, and the fact that our analysis was conducted on national averages, may offset local impacts of precipitation change on

agricultural N use and loss. However, there is very limited high-resolution data of agricultural N use and loss available over a long time period (1961–2018) to support such an analysis with a sufficiently high spatial resolution to identify the effect of precipitation change at local scale. Thus, the effect of precipitation changes on agricultural N use and loss may underestimate local scale variations, but we are confident that our national scale analysis remains meaningful, since food security objectives and environmental policies are typically organized at national scale. And the implement of national policies will be adequately adapted to local circumstances at specific regional scales.

Non-linear response to climate change

The primary mechanism driving the spatial variability of N use and loss can be attributed to non-linear responses of key parameters to climate change. Air temperature change relates to crop yield following an inverted-U shape (Table 1, Extended Data Fig. 2) and the turning point is calculated at approximately 9.3 °C (Extended Data Table 1). Temperature near the turning point is beneficial to reach a high crop yield. In countries with an average temperature below 9.3 °C, warming will increase crop yield, such as in Canada, Russia and countries in the HMNH. But when the temperature exceeds the turning point, there will be a negative effect on crop yield, for example, countries from the LSH. The higher the temperature increase, the larger the yield loss. This may be due to the fact that crops grown at higher latitudes, such as wheat, are more adapted to temperature increases, hence yield improvements can be observed under global warming conditions in these regions^{17,18}. There is a U-shaped relationship between temperature and fertilization with a turning point at approximately 24.3 °C that most countries are not reaching (Table 1 and Extended Data Table 1). It means current air temperature increase would significantly reduce fertilization across most of the countries.

The non-linear responses of yield and fertilization caused by temperature changes further affect cropland NUE. An inverted-U shape between temperature and cropland NUE is observed with the turning point at 10.2 °C. For most countries in the HMNH, global warming is expected to contribute to an NUE increase given their average temperature is before the turning point. In contrast, global warming is projected to reduce NUE in warmer countries since their temperature has passed the turning point.

While there are no clear trends for precipitation at a global scale, large variations are projected for different years. The effect of precipitation on yield and NUE is similar to temperature following an inverted-U relationship (Table 1, Extended Data Fig. 2). It indicates that precipitation in a moderate range (about 2,600 mm of annual precipitation) is beneficial to yield and NUE (Extended Data Table 1). However, extreme precipitation events (far away from the turning point, too much or too little precipitation) and their spatial variability usually lead to floods and droughts, which could substantially reduce agricultural yield and cropland NUE. However, the standardized coefficients for precipitation effects on fertilization and NUE are smaller than those for temperature, indicating its relatively small impact compared to temperature on national average scale (Extended Data Table 2).

Moderate temperature and precipitation can benefit crop yield, which is partly attributed to an increase in photosynthesis. Extremes in temperature and precipitation could destroy the growth environment of crops, reduce their N uptake and then lowered their yields¹⁹. Global warming often causes dry and hot extremes at the same time³, which leads to farmers reducing fertilizer input to cropland as the average temperature rising. Irrigation can alleviate the negative impact of yield and fertilization caused by global warming^{20,21}. But there

are still gaps for irrigation to compensate for these adverse effects^{21,22}. Thus, it can still be observed that temperature rising reduces agricultural N yield and fertilization even we take the impact of irrigation into consideration (Table 1). In addition to fertilizer and yield, climate change also affects the NUE in other pathways. For example, climate change increases N losses from croplands by aggravating gas emissions such as NH₃²³; extreme rainfall intensifies soil erosion, taking away N in cropland soil and reducing NUE^{19,24}. Climate change may also play a critical role in the rate of biological N fixation^{25,26}.

Changes of CAPRP intensify spatial variability

CAPRP shows a significantly positive correlation with cropland NUE, but negative with N fertilization (Table 1). Large CAPRP implies that more cropland area is managed per rural population, and is thus strongly and positively connected with large-scale farming (Table S1). Farms in countries with large CAPRP are usually equipped with improved agricultural practices such as better infrastructure, including drainage and irrigation facilities, which can increase NUE while maintaining or increasing crop yields^{27,28}. Even in the absence of sufficient infrastructures in some developing regions, increase in CAPRP encourages farmers to have better knowledge than benefits their ability to adapt to climate change to minimize negative impacts¹⁶. This could explain why CAPRP appears to enhance NUE while reducing N surplus. Large CAPRP is mainly due to abundant cropland resources or a small rural population. Economically developed countries with high urbanization usually have higher CAPRP and larger farms, as a large proportion of rural people has migrated to urban areas^{29,30}. In contrast, countries with small CAPRP are vulnerable to climate change due to limited resources, low GDP per capita and a lack of agricultural facilities and knowledge. Even in the countries with middle-level economies such as China, the small CAPRP lead to dominated smallholder farming with limited facilities and knowledge, which in turn affects adaptation to climate change.

Global average CAPRP has declined since 1961 mainly due to the increase of rural population, but rebounded from 1990s due to urbanization (Extended Data Fig. 3a). As a result, global cropland NUE has been further reduced compared to that under climate change effects, despite the trend increasing after the 1990s (Fig. 2g, h, i). And N fertilization is turned to increase from decrease affected by changes in CAPRP, especially from the 1980s to the 2000s (Fig. 2c, f, l). CAPRP has a positive but not statistically significant relationship with cropland N yield (Table 1). It has been proved that CAPRP has no significant impact on agricultural production which is in line with our findings³¹. The correlation is, however, positive, indicating that increasing CAPRP can boost cropland N yield slightly. Thus, cropland N yield has increased in comparison to climate change effects (Fig. 2a, b, c). Consequently, N surplus has been reduced with CAPRP, based on the significant relationship with NUE and N yield. That means, compared to small CAPRP, farming under large CAPRP could reduce N surplus (Fig. 2j, k, i).

CAPRP has increased in about 35% of countries globally compared to 1961, including China, some South American and Europe countries (Extended Data Fig. 3b). Significant NUE improvements, and N fertilization and surplus reductions can be found in these countries (Fig. 3f, i, l). For example, climate change reductions in NUE are offset by an increase in CAPRP in Brazil in 2018, which also leads to a decrease in fertilizer use by 38% compared to climate results, yield and NUE improvement by 2.3% and 13%, respectively, and N surplus declines by 53%. The remaining 65% of countries, however, showed a reduction of their CAPRPs, which has aggravated the negative impacts of climate change, especially in Africa and Middle East. Cropland NUE reduction has been

further increased from 3% to 16% due to CAPRP decline in Sub-Saharan Africa. Similar results can be observed in fertilization from increase 0.4% to 12%, leading to N surplus increased to 18% from 7% and N yield loss increased by 0.5% in 2018. Generally, CAPRP changes further improved NUE in Asian and European countries in the HMNH and reversed NUE reduction in Latin American countries in LSH. However, reduction of cropland NUE in the remaining countries in the LSH was aggravated and the positive effects of climate change on NUE were weakened in North America. These uneven changes in CAPRP further exacerbate the global trend of N use and loss inequalities.

There is diverging farming performance between small and large CAPRPs regarding N use and loss under climate change conditions. NUE changes due to changes in climate tend to be much smaller under large CAPRP (> 1 ha) compared to small CAPRP (\leq 1 ha) (Fig. 4a, b), indicating a higher degree of vulnerability under limited CAPRP from climate change. Large CAPRP in contrast contributes to NUE improvements, while reducing N fertilization and N surplus. Meanwhile, measures to enable adaptation to climate change are different for large and small CAPRPs, illustrated by the significance of CAPRP and its interaction items with climate change indicators in regression results (Table 1). To quantify the relative contribution of climate change effects and CAPRP on N use and losses in global croplands, we estimated the standardization coefficient of the explanatory variables in both small and large CAPRP groups based on regression of 1961 to 2018 (Fig. 4c, d). Results show that effect from CAPRP change in the large CAPRP group can reverse the decline in NUE and the increase in surplus while maintaining N yield. In contrast, the effect from CAPRP change is much smaller in the small CAPRP group. Analyzing the combined effects of climate change and CAPRP, a reduction of NUE and an increase in surplus are still found in the small CAPRP group.

In this paper, we used harvested N per ha to represent crop yield, which is positively correlated to CAPRP. It may be interpreted as the result of improved seeds, more targeted N fertilizer application, scientific and technologically supported farm management and advanced technology under large CAPRP and large-scale farming. However, the effects of CAPRP can vary substantially across global regions (Extended Data Fig. 4). We incorporated the quadratic term of CAPRP in regression analysis and found that it has an inverted U-shaped relationship with NUE (Table S2). The turning point is estimated to be 90 ha on average even though the global average CAPRP is 1.0 ha (0-12.5 ha) in 2018 (Extended Data Table 1). This indicates that an increase in CAPRP promotes NUE globally. That also explains why we observe a significant positive association between CAPRP and NUE, but not with its quadratic term (Table S2). Similarly, increasing CAPRP reduces N fertilizer overapplication when CAPRP is less than 11 ha, but it may further increase the application when exceeding 11 ha (Extended Data Table 1). As a result, only a moderate rise in CAPRP, based on local factors such as technical levels and management capabilities, could contribute to climate change adaptation. Further increases in CAPRP may intensify the detrimental impact of climate change on cropland N use in countries where already have large CAPRP such as USA and Australia.

Managing croplands to offset climate impact

Global average NUE changes under different SSP scenarios would be decreasing slowly if temperature increase continues towards 2100 (Extended Data Fig. 5e). However, substantial spatial variability further diverges between colder countries in the HMNH and warmer countries in LSH in 2100. Even under the optimum scenario (SSP1) with a projected temperature increase by 3.0 °C by 2100 compared to pre-industrial level, yield and NUE would be further reduced in warmer countries in the LSH compared to the observed in 2018 (Fig. 5, Fig. S2).

Yield decreases are averaged at 6% (0-15%) projected for 94% of countries globally in 2100, mainly distributed in LSH. NUE decline will be further aggravated, especially in Africa, South and Southeast Asia and Latin America, which already have low NUE (Extended Data Fig. 6). N surplus will further worsen in the Southern Hemisphere, aggravating N pollution in Australia and Brazil (Fig. 5). In contrast, increase projected in North America and Former Soviet Union would strengthen their already high NUE and yield, and low N surplus (Extended Data Fig. 6). These variations will exacerbate the national inequalities on agricultural N use and loss in the future. In the worst-case scenario (SSP3) with global average temperature increasing by 4.1 °C in 2100, these impacts would be diverging more seriously globally (Extended Data Fig. 7, Fig. S3). It will substantially change the current pattern of N use, aggravating the inequalities on food production and agricultural environmental protection.

Improving farmers' practices through managing CAPRP appropriately is a critical path for climate adaptation to ensuring food security and reduce agriculture pollution while eliminating their national inequalities. In the optimum (SSP1) scenario, the global average urbanization rate will exceed 90% by 2075 and reach up to 93% by 2100. That means that a large number of the rural population will move to urban areas, leading to the increase of large-scale farming²⁹. As a result, the declining trend of cropland NUE over time will be reversed, projected to increase from 45% in 2018 to 60% in 2100, with a 1% yield loss, 49% fertilizer reduction and 44% decline of N surplus compared to the observed in 2018 (Extended Data Fig. 5). More importantly, the spatial variability of NUE changes due to global warming could be balanced through better management with NUE improvements across all countries (Fig. 5) and eliminating the national inequalities.

Even in the SSP3 scenario with an average urbanization rate of only 70% in 2100, the global average NUE increases to 48% (Extended Data Fig. 5), including the effect of CAPRP change. However, the fertilization will decrease by only 21%, and N surplus will decline by 13%. That is mainly due to the unbalanced development leading to the diverging trends of CAPRP across different countries. In developing regions such as Africa, South and southeast Asia, average CAPRPs would decline substantially. This will result in more yield and NUE reduction, then increase N surplus. In sub-Saharan Africa, NUE decreases by an average of 15% and N surplus increases by 18% in 2100 compared to 2018 (Extended Data Fig. 7, Fig. S3). The declining trend of NUE and the increase trend of N surplus due to rising temperature would be reversed through enlarging CAPRP in these smallholder-dominated countries.

Enlarging CAPRP can reduce spatial variability on agricultural N use and loss caused by climate change and reduce national inequalities under SSP1 scenario. Many farms around the world show promise for achieving sustainable management, but are limited by farm scales³². Improving CAPRP moderately then benefiting farmer' practices has been a critical and significant task. Promoting CAPRP involves multiple stakeholders, including government, farmers, social organizations etc.³². Establishing an N credit system for these stakeholders presents a viable path to improve NUE and reduce N losses³³. Urbanization is also having a profound impact on the release of more croplands and reduction of rural population, benefiting CAPRP increase and large-scale farming^{29,34}. Moreover, training and better agricultural facilities and technologies are also effective measures to enable adaptation to the adverse effects of climate change³⁵. Improving cropland NUE and managing cropland sustainably would in turn slow down the rise in temperature rising reduction of greenhouse gas emission from agriculture^{36,37}. Thus, early actions should be taken to ease the projected future impact of climate change on agriculture to achieve the global sustainable goals^{38,39}.

Additionally, it's worth emphasizing that enlarging CAPRP must be promoted appropriately based on local circumstances. Even though turning points for N use and loss were measured (Extended Data Table 1), these points may change depending on regional conditions. In particular, cautions are needed to manage CAPRP to adapt climate change in countries where already have large CAPRP, and reducing farm size to an optimal level may be helpful given the inverted U-shaped relationship of CAPRP with N use and loss. Meanwhile, large-scale farming favored by large CAPRP has certain negative consequences, such as biodiversity loss, soil erosion, and nutrient loss⁴⁰⁻⁴². When dealing with market fluctuations, the possibility of large-scale farms, especially for industrial farms, encountering unfavorable consequences would grow, putting negative pressure on the economy and causing financial problems^{43,44}. Accordingly, CAPRP should be promoted in compliance with the relevant natural and socioeconomic conditions in order to maximize its value to achieve agricultural and environmental sustainability and eliminate national inequalities on food production and agricultural pollution control.

Methods

Data sources and data processing. Data used in this study are mainly collected from the Food and Agriculture Organization online statistical databases of the United Nations (FAOSTAT) (<http://www.fao.org/statistics/databases/en/>). FAOSTAT provides comprehensive and standardized agricultural and socioeconomic data all over the world from 1961 to the most recent year available. In this paper, the calculation of cropland fertilization and yield, NUE, cash crop ratio, cropland area per rural population (CAPRP), and the gross domestic product per capita (PGDP) are based on agricultural production, fertilization (including synthetic fertilizer and manure), irrigation, land use, population, and so on.

The average country-level farm size data is derived from Lowder et al., 2014³⁰. It is the average of farmers' actual operating agricultural land area. The relationship of the CAPRP and the actual farm size is listed in Table S1.

Dataset for global inorganic N deposition at a spatial resolution of $2^\circ \times 2.5^\circ$ was derived from Ackerman et al., 2019⁴⁵. Information on global irrigation management was derived from the FAO's Global Information System on Water and Agriculture (<http://www.fao.org/aquastat/en/>).

Historical observations of climatic data, including the mean air temperature, total precipitation, and atmospheric carbon dioxide (CO₂) concentration, were considered in our analysis. The monthly temperature (°C) and precipitation (mm/month) from January 1961 to December 2018 were derived from the Centre for Environmental Data Analysis (CEDA) global climatic dataset at $0.5^\circ \times 0.5^\circ$ spatial resolution (Available online: <http://badc.nerc.ac.uk>). The Atmospheric Infrared Sounder (AIRS) monthly carbon dioxide concentration (ppm) at a spatial resolution of $2.5^\circ \times 2^\circ$ from September 2002 to February 2017 was derived from the Goddard Earth Sciences Data and Information Services Center (GES DISC) (Available online: <https://disc.gsfc.nasa.gov/>). For each selected country, the climatic variables were sampled by nearest neighbor assignment according to the boundary and averaged by month.

And we also obtained the simulated counterfactual monthly climate data with and without climate change from Ortiz-Bobea et al., 2021⁴⁶. Data are fully provided at the Cornell Institute for Social and Economic

Research (CISER): <https://doi.org/10.6077/pfsd-0v93>. We averaged their monthly bias-corrected data of seven general circulation models (GCMs) from the ‘hist-nat’ and the ‘historical’ experiment as weather data with and without climate change, respectively.

We obtained country-level rural population and average global temperature increase data based on the Shared Socioeconomic Pathways (SSP) database hosted by the IIASA Energy Program (<https://tntcat.iiasa.ac.at/SspDb>). The country-level rural population was obtained to calculate CAPRP. CAPRP and temperature changes under different SSP scenarios are presented in Extended Data Fig. 8. In this paper, we only consider three SSP scenarios with low (SSP1), intermediate (SSP2), and high developing challenges (SSP3), respectively.

Nitrogen budget. This study compiled the global cropland N budgets at a national scale from 1961 to 2018 based on the Coupled Human And Natural Systems (CHANS) model. CHANS is a N mass balance model which combines bottom-up N input and output fluxes among 14 subsystems (cropland, livestock, grassland, forest, aquaculture, industry, human, pet, urban green land, wastewater treatment, garbage treatment, atmosphere, surface water, and groundwater) and top-down reactive N fluxes datasets on different (regional, national, global) scales to provide a comprehensive understanding of N cycling and fluxes⁴⁷. A detailed model introduction can be found in Zhang et al., 2017⁴⁸ and Gu et al., 2015⁴⁷. In this study, the cropland system is identified as the subject in CHANS covering all crops across the year, the calculation of cropland N budget in each country is formulated in Eq. (1–3):

$$N_{input,i} = N_{fer,i} + N_{man,i} + N_{fix,i} + N_{dep,i} + N_{irr,i}$$

1

$$N_{output,i} = N_{harvest,i} + N_{gas,i} + N_{runoff,i} + N_{leaching,i}$$

2

$$NUE_i = \frac{N_{harvest,i}}{N_{input,i}}$$

3

where $N_{input,i}$ is the total N inputs to the cropland across all crops in the country i , include synthetic fertilizer application ($N_{fer,i}$), manure application ($N_{man,i}$), biological fixation ($N_{fix,i}$), atmospheric deposition ($N_{dep,i}$), and irrigation ($N_{irr,i}$). $N_{output,i}$ is the total N outputs from the cropland, include crop harvest ($N_{harvest,i}$, the sum of the yield of each crop multiplied by their N content), N gas emissions ($N_{gas,i}$, including NH_3 , N_2 , N_2O and NO_x emissions), riverine runoff ($N_{runoff,i}$), and leaching to groundwater ($N_{leaching,i}$). The estimates of different N outputs from croplands are based on parameters and emission factors nested in the CHANS model. NUE (NUE_i) is defined as the ratio of harvest N to total N inputs in cropland system in country i . Accordingly, we derived yield (kg N ha^{-1}) in each country using crop harvest N divided by the total harvest area. And fertilization (kg N ha^{-1}) is the ratio of the sum of N content in synthetic fertilizer application to the total harvest area. Surplus (kg N ha^{-1}) is the difference between the harvest N and total N inputs of the cropland system per area. Due to the effect of the interaction of a variety of crops during rotations on NUE, we aggregated data on

all crops instead of investigated individual crop in this study. At the same time, there is insufficient data of agricultural N use and losses for each crop individually for all countries or on subnational scale for such a long study period.

Statistical analysis. To estimate the response of agricultural N yield, fertilization, NUE and surplus to climate change and CAPRP changes, we used a fixed-effect model to do panel analysis while controlling for compounding factors such as crop type. We estimated the following equation using country-level data from 1961 to 2018:

$$\begin{aligned} \ln Y_{it} = & \alpha + \beta \cdot \ln CAPRP_{it} + \gamma_1 \cdot T_{it} + \gamma_2 \cdot T_{it}^2 + \delta_1 \cdot P_{it} + \delta_2 \cdot P_{it}^2 + \theta_1 \cdot \ln CAPRP_{it} \\ & \cdot T_{it} + \theta_2 \cdot \ln CAPRP_{it} \cdot T_{it}^2 + \theta_3 \cdot \ln CAPRP_{it} \cdot P_{it} + \theta_4 \cdot \ln CAPRP_{it} \\ & \cdot P_{it}^2 + \sum_n \varphi_n q_{nit} + \sigma_i + \varepsilon_t + \mu_{it} \end{aligned} \quad (4)$$

where the subscript i and t denotes country and year, respectively. Y_{it} are explained variables, namely, yield, fertilization, NUE and N surplus. $\ln CAPRP$ is the logarithm of the cropland area per rural population. T and P are the abbreviations of the average temperature (10^2 °C) and total precipitation (10^4 mm) across the year, respectively. T^2 and P^2 are their quadratic terms. We also introduced the interaction items of T , P , T^2 and P^2 with $\ln CAPRP$ to explore how CAPRP can change nitrogen use and loss under climate change. q_n is control variable, including crop type, cash crop ratio, and irrigation. α is a constant, σ_i , ε_t and μ_{it} are error items. β , γ , δ , θ and ϕ are coefficients that need to be estimated.

We include a country-level intercept σ_i to control for time-invariant factors (unobserved heterogeneity) that may skew the estimation, such as country area, topography and soil conditions, political background, local facilities and planting culture etc. In addition, we include time fixed effects ε_t to control for time trends that are common across all countries such as financial crisis. Besides, we set other controlling variables including cash crop ratio, crop type, and irrigation. The cash crop ratio is the harvest area of cash crops divided by the total harvest area, which has been proven as a critical driver substantially affecting the country-level N use⁸. Crop type is a categorical variable denoting the main type of crop the country grows. We mainly focus on eleven crop types referring to crop categories of FAOSTAT in our regression analysis, including rice, wheat, maize, other cereals, soybeans, other oil crops, pulses, sugar crops, roots and tubers, vegetables and fruits, and other crops. And the crop type of each country in each year is determined by which crop's sowing area exceeds all other crops. For example, if the sowing area of rice exceeds that of any other crop, the main crop type of this country is rice. Irrigation is a binary variable (equaling to 1 and 0 if there is or no irrigated land, respectively). The reason why we set control these variables is to observe the net relationship between independent and dependent variables under same conditions. For example, crop type is controlled with the purpose that the relationship between dependent and independent variables can be derived under same crop type. In other word, our conclusions in this paper are all derived after considering the effect on crop type. Besides, in the equations whose explained variable is yield and NUE, fertilization is further controlled.

The model incorporates country time-invariant controls and year fixed effects, as are usual standard practices in the literature concerning climate change and agriculture. To separate the impact of exogenous changes in temperature and precipitation on agricultural N use and loss, these controls must be considered. However, one drawback of the fixed effect model is that they might absorb a lot of weather change. Table S6 shows the R-square and standard deviation of residual seasonal weather variance that is not absorbed by various sets of fixed effects. For instance, merely having year fixed effects preserves a large amount of temperature variance, but including country fixed effects significantly reduces the remaining variation, implying that geographical differences account for the majority of temperature variation. To account for within-country clustering of errors and arbitrary correlation of observations across time, cluster-robust standard errors are used⁴⁴. The results are detailed in Table 1 and summary statistics are in Table S3. The within R² in the tables refers to the fraction of variance in the outcome that is explained by the climatic variables after time-invariant factors are considered.

We did the statistical analysis in Stata16.0 software.

Impact of climate change and CAPRP. We calculated the impact of global warming (temperature change), climate change (temperature and precipitation change) by subtracting the N counterfactual value without climate derived using the simulated weather data change from the observed N value subject to climate change. The simulated weather data with and without climate change were averaged across seven GCMs⁴⁶. The combined impacts of climate and CAPRP change (CCPC) were further assessed assuming the CAPRP remains unchanged from 1961. CAPRP change is the amount of change compare to 1961. For country i , the impact is calculated according to the following equation:

$$\text{Ln}Y_{it} = \alpha + \beta \bullet \text{LnCAPRP}_{it} + \gamma_1 \bullet T_{it} + \gamma_2 \bullet T_{it}^2 + \delta_1 \bullet P_{it} + \delta_2 \bullet P_{it}^2 + \sum_n \phi_n q_{nit} + \sigma_i + \epsilon_t + \mu_{it}$$

5

where the subscript i and t denotes country and year, respectively. Y_{it} are explained variables of N use and loss, namely, yield, fertilization, NUE and N surplus. LnCAPRP is the logarithm of the cropland area per rural population. T and P are the abbreviations of the average temperature (10² °C) and total precipitation (10⁴ mm) across the year, respectively. T^2 and P^2 are their quadratic terms. q_n is control variable, including cash crop ratio, and irrigation. α is a constant, σ_i , ϵ_t and μ_{it} are error items. β , γ , δ and ϕ are coefficients that need to be estimated. And year and country fixed effects are also be included. In the equations whose explained variable is yield, NUE, and N surplus, fertilization is further controlled. Regression results are in Table 1.

Based on coefficients estimated in Eq. (5), we first calculated the differences of explained variables of N use and loss between the weather with and without global warming (GW) on each country as follows:

$$\Delta \text{Ln}Y_{it}^{GW} = \gamma_1 \bullet \Delta T_{it} + \gamma_2 \bullet \Delta T_{it}^2$$

(6)

ΔT_{it} refers to temperature difference of weather with and without climate change. Accordingly, the differences of explained variables of N use and loss between the weather with and without climate change (CC) on country-level was calculated as follows:

$$\Delta \ln Y_{it}^{CC} = \gamma_1 \cdot \Delta T_{it} + \gamma_2 \cdot \Delta T_{it}^2 + \delta_1 \cdot \Delta P_{it} + \delta_2 \cdot \Delta P_{it}^2$$

(7)

ΔT_{it} refers to temperature difference of weather with and without climate change. Similarly, ΔP_{it} is the precipitation difference. Then the differences of explained variables of N use and loss between with climate and CAPRP changes and without climate and CAPRP changes (CCPC) was calculated as follows:

$$\Delta \ln Y_{it}^{CCPC} = \beta \cdot \Delta \ln CAPRP_{it} + \gamma_1 \cdot \Delta T_{it} + \gamma_2 \cdot \Delta T_{it}^2 + \delta_1 \cdot \Delta P_{it} + \delta_2 \cdot \Delta P_{it}^2$$

(8)

$\Delta \ln CAPRP_{it}$ means the CAPRP change for country i in year t compared to 1961.

We then add that difference $\Delta \ln Y_{it}$ to the actual observed N use and loss $\ln Y_{it}$ to calculate the counterfactual values:

$$Y_{it}^{WithoutGW} = \exp(\Delta \ln Y_{it}^{GW} + \ln Y_{it})$$

(9)

$$Y_{it}^{WithoutCC} = \exp(\Delta \ln Y_{it}^{CC} + \ln Y_{it})$$

(10)

$$Y_{it}^{WithoutCCPC} = \exp(\Delta \ln Y_{it}^{CCPC} + \ln Y_{it})$$

(11)

Finally, the impact is the difference between the actual observed value and the counterfactual value:

$$Impact_{it}^{GW} = Y_{it} - Y_{it}^{WithoutGW}$$

(12)

$$Impact_{it}^{CC} = Y_{it} - Y_{it}^{WithoutCC}$$

(13)

$$Impact_{it}^{CCPC} = Y_{it} - Y_{it}^{WithoutCCPC}$$

(14)

When we calculate the impact of global warming, only temperature difference is considered. The impact of climate change is considering both temperature and precipitation changes. The combined impacts of climate and CAPRP changes incorporate temperature, precipitation and CAPRP differences. Note that we first derived the impact on fertilization. Then yield and NUE was derived further considering fertilization impact as it is one

of the explanatory variables. The impact of N surplus was finally calculated, which is the difference between predicted harvest N and total N input then divided by harvest area. The predicted harvest N is calculated by multiplying the harvest area by the N yield. Total N input was derived according to N yield and NUE based on Eq. (3). Global weighted-mean values of country-level impacts from 1961 to 2018 are shown in Fig. 2. N yield, fertilization and surplus were weighted by national harvest area; NUE was weighted by total cropland N input in each country.

To reflect the joint statistical uncertainty from the econometric model and climate uncertainty, we calculated the impacts for 5,000 random pairs of bootstrapped coefficients for Eq. (5). The upper and lower limits of estimated coefficients can be computed using a 90% confidence zone. Using the upper limits of estimated coefficients, the upper limit of impacts can be derived. The lower limit of impacts can also be computed using the estimated coefficients' lower limits. The global results based on bootstrapping are presented in Fig. 2. The country-level results are in Fig. S4 and S5, which reveals the uncertainty in exactly which countries are likely to benefit or be penalized by climate and CAPRP change. The results in Figs. S4 and S5 show that our main conclusion that climate change would boost NUE in the Northern Hemisphere's high and middle latitudes while decreasing NUE in the remaining countries holds robust for both the upper and lower limit estimations. Similarly, the conclusions for N fertilizer and surplus hold robust, despite some uncertainty in the yield results.

Additionally, we consider standardized coefficient estimations, which allow us to compare coefficients of models with different dependent and independent variables. For standardization, we utilize the standard deviation of the fixed effects residuals. The coefficients can be interpreted as standard deviation changes in N use and loss with a one standard deviation change in the respective climatic factor. Results are presented in Extended Data Table 2.

Robust checks. Since carbon dioxide (CO₂) concentration is also a common indicator describing global warming, we further took annual CO₂ concentration (ppm) into consideration for a robust check. As CO₂ and temperature are highly correlated with over 0.99 of R-square (Table S5), temperature is removed in this analysis. We estimated the following equation using country-level data from 2002 to 2018:

$$\ln Y_{it} = \alpha + \beta \cdot \ln CAPRP_{it} + \gamma_1 \cdot CO_{2,it} + \gamma_2 \cdot CO_{2,it}^2 + \sum_n \phi_n q_{nit} + \sigma_i + \epsilon_t + \mu_{it}$$

15

where the subscript i and t denotes country and year, respectively. Y_{it} stands for explained variables, namely, yield, fertilization, NUE, and N surplus. $\ln CAPRP$ is the logarithm of the cropland area per rural population. CO_2 is the abbreviations of carbon dioxide (averaged by monthly CO₂ concentration data) and CO_2^2 represents its quadratic term. We didn't introduce their interaction items with $\ln CAPRP$. Because we consider CO₂ concentration changes are long-term and not dramatic, which is not easy to be noticed by farmers. Thus, farmers would not change their management to deal with CO₂ concentration changes, leading to no interaction effects with CAPRP. q_n is control variable, including the total precipitation and its quadratic term, cash crop ratio, crop type and irrigation. And year and country fixed effects are also be included. In the equations whose explained variable is yield and NUE, fertilization is further controlled. α is a constant, σ_i and μ_{it} are error items. γ and ϕ are coefficients that need to be estimated. Results in Table S6 shows that temporal

differences account for the majority of CO₂ variation. Cluster-robust standard errors on year level is added when analyzing the effects of CO₂ (Table S4). The results are detailed in Table S4 and summary statistics are in Table S3. The relationship between precipitation, CAPRP and N use and loss showed in Table S4 is the same as the results in Table 1. Although there are some changes in the significance, the robustness of the results can be derived.

Besides, based on formula (4) and (5) in the main manuscript, we further added the country-level PGDP and its quadratic term (results in Table S6). PGDP is a typical indicator representing economic development and technology level. The aim is to test the robustness of our main findings when further considering the role of economic development and technology. All results have no significant change, which proves the robustness of the response of climate change and CAPRP to N use and loss. As PGDP is correlated with urbanization and CAPRP, the significance of the independent variables in Table S6 may be impacted. Thus, PGDP was not considered in the main regression models in Table 1.

Scenario analysis. We considered three SSP scenarios (SSP1, SSP1, and SSP3 with low, intermediate, and high developing challenges, respectively) to conduct scenario analyses to see how the agricultural yield, fertilization, NUE and N surplus would change if global warming and CAPRP changes continue. SSP1 is the sustainable and “green” pathway with high urbanization and reduced national economic inequalities, which the global temperature will increase 3.0°C by 2100 compared to the pre-industrial level. SSP2 is the “middle of the road” or medium pathway extrapolating the past and current global development into the future. Income trends in different countries are diverging significantly and global population growth is moderate. The global temperature increase will be up to 3.8 °C by 2100. Under SSP3, a revival of nationalism and regional conflicts pushes global inequality to rise. Global population growth is the largest among these three scenarios. And the global temperature increase will be up to 4.1 °C by 2100. The temperature and CAPRP changes under SSPs are depicted in Extended Data Fig. 8.

First, we obtained regional cropland area, country-level rural population and average global temperature increase data (2010–2100) from the SSP database. Based on the ratio of the country- to region-level cropland area in 2010 from the FAO database, we weighted the 2020–2100 regional data and developed a future country-level cropland area. And country-level CAPRP was calculated further using the rural population from 2020 to 2100. Then we got the changes of CAPRP compared to 2018. Meanwhile, the average global temperature increase from pre-industrial has been converted to the increase compared to 2018. We firstly calculated the contribution of each country's temperature increase to global average temperature change from 2009 to 2018 based on weather data with and without climate change averaged from seven GCMs. Then each country's temperature increase towards 2100 under SSP scenarios was projected by multiplying the country-level contribution and global temperature increase. In this process, we also compared the global average temperature increase from 2005 to 2010 and rural population data from CEDA and FAOSTAT, respectively, with the data from the SSP database. Accordingly, we weighted the scenario temperature increase and rural population proportionally to reduce the error caused by different databases. Then the yield, fertilization and NUE trend were derived based on Eq. (5)-(14) as follows:

$$\Delta \text{Ln}Y_{it}^{SSP} = \beta \bullet \Delta \text{Ln}CAPRP_{it} + \gamma_1 \bullet \Delta T_{it} + \gamma_2 \bullet \Delta T_{it}^2$$

$$Y_{it}^{SSP} = \exp \left(\text{Ln}Y_{i,2018}^{Observed} + \Delta \text{Ln}Y_{it}^{SSP} \right)$$

(17)

$$\text{Change}_{it}^{SSP} = Y_{it}^{SSP} - Y_{i,2018}^{Observed}$$

(18)

Note that Δ refers to the value difference between year i and 2018. Y_{it}^{SSP} is the simulated value under SSP scenarios.

Similarly, we first derived the impact of fertilization. Then yield and NUE was derived based on predicted fertilization as it is one of the explanatory variables. The impact of N surplus was finally calculated. Note that global means of N yield, fertilization and surplus were weighted by national harvest area (Extended Data Fig. 5). And global average NUE was weighted by total cropland N input in each country. The relative changes of N yield, fertilization, NUE and N surplus in 2100 under SSP1, SSP2 and SSP3 are in Fig. 5, Extended Data 5 and Fig. S6, respectively. The physical changes under SSP1, SSP2 and SSP3 are in Fig. S2, S3 and S7, respectively.

Limitations. Our study has some limitations that are crucial to consider when interpreting our findings. The main objective of this study was to assess the effects of climate change and CAPRP on N use and loss on cropland. Despite the fact that this study includes a large sample of 150 countries and spans nearly 60 years of data, the precision is limited to the national and annual scales. The heterogeneity of climate change, N use and losses within a country was not captured, even though cluster-robust standard errors are used, especially for countries which span large geographical areas like China, Russia, and USA. However, the findings of the non-linear relationship between agricultural yields and temperature and precipitation in our study, which used country- and annual-level data, are in line with earlier research^{17,49,50}. Furthermore, scientific evidence indicates that the yields of wheat, rice, and soybeans would increase in high latitudes due to climate change by the end of this century, but remain large uncertainties low latitudes¹⁷. And climate change has harmed the yields of the majority of agricultural crops in low latitudes, whereas high latitudes have potential gains¹⁸. Both studies investigated how global individual crops respond to climate change, and the results are highly consistent with our estimates. This implies that while conducting the analysis at this coarse scale may add some inaccuracies, the essential results on national scale are robust and valid. In addition, while we derived conclusions controlling for crop type, we did not adequately investigate the response of specific crops to N use and losses as a result of climate and CAPRP change. The conclusions we reached lacked empirical evidence in terms of crop responses. To completely capture the underlying motivations and mechanisms beyond what we can study with our data, more work is needed, particularly at more disaggregated spatial scales as well as crop types.

The type of counterfactual scenarios we use, as well as the model design, influence our outcomes. Although we include year and country fixed effects to predict N use and loss under counterfactual scenarios, we cannot account for feedbacks of variables such as abrupt land cover changes within countries, which may alter the relationship between climate change and N indicators, like other statistical models. In addition, of data

obtained from seven GCMs to establish counterfactual scenario, we only used one average value rather than developing the analysis for each of the seven models, which may also introduce some computational bias.⁴

Despite these limitations, this research contributes to advancing the scientific understanding of how climate change, global agricultural food security, environmental protection, and spatial aspects of N use and losses are connected. We established cross-regional comparability and build a unique cross-regional dataset needed for the research by using uniform N variables to indicate food production and environmental pollution. The interactions of CAPRP and climate is critical for addressing climate change and maintaining food security, then achieving global sustainable development goals such as ending hunger, reducing inequalities, and sustaining the environment.

Declarations

Data availability

Data supporting the findings of this study are available within the article and its supplementary information files. All data are publicly available and open access.

Acknowledgements

This study was supported by the National Natural Science Foundation of China (42061124001, 41822701 and 41773068).

Author contributions

B.G. designed the study. C.R. conducted the research. B.G., and C.R. wrote the first draft of the paper, X.Z., and S.R. revised the paper. X.Z., and J.X. processed the raw data. And all authors contributed to the discussion and revision of the paper.

Declaration of competing interest

All authors have no conflicts of interest to report.

References

1. Revel, D. Climate change 2014: synthesis report. (Veille énergie climat, 2014).
2. Kirchmeier-Young, M.C. & Zhang, X. Human influence has intensified extreme precipitation in North America. *Proc. Natl. Acad. Sci. U. S. A.* **117**, 13308–13313 (2020).
3. Alizadeh, M.R., *et al.* A century of observations reveals increasing likelihood of continental-scale compound dry-hot extremes. *Sci. Adv.* **6**, z4571 (2020).
4. Xu, C., Kohler, T.A., Lenton, T.M., Svenning, J. & Scheffer, M. Future of the human climate niche. *Proc. Natl. Acad. Sci. U. S. A.* **117**, 11350–11355 (2020).
5. Zhao, C., *et al.* Temperature increase reduces global yields of major crops in four independent estimates. *Proc. Natl. Acad. Sci. U. S. A.* **114**, 9326–9331 (2017).

6. Erisman, J.W., Sutton, M.A., Galloway, J., Klimont, Z. & Winiwarter, W. How a century of ammonia synthesis changed the world. *Nat. Geosci.* **1**, 636–639 (2008).
7. Steffen, W., *et al.* Planetary boundaries: Guiding human development on a changing planet. *Science* **347**, 1259855 (2015).
8. Zhang, X., *et al.* Managing nitrogen for sustainable development. *Nature* **528**, 51–59 (2015).
9. Oene, O., *et al.* *Nitrogen Use Efficiency (NUE) - an indicator for the utilization of nitrogen in agriculture and food systems Prepared by the EU Nitrogen Expert Panel* (2015).
10. Reay, D.S., *et al.* Global agriculture and nitrous oxide emissions. *Nat. Clim. Chang.* **2**, 410–416 (2012).
11. Sutton, M.A., *et al.* Towards a climate-dependent paradigm of ammonia emission and deposition. *Philos. Trans. R. Soc. B-Biol. Sci.* **368**, 20130166 (2013).
12. Huang, X., *et al.* A high-resolution ammonia emission inventory in China. *Glob. Biogeochem. Cycle* **26**, B1030 (2012).
13. Sun, Y., *et al.* The Warming Climate Aggravates Atmospheric Nitrogen Pollution in Australia. *Research* **2021**, 1–12 (2021).
14. Sinha, E., Michalak, A.M. & Balaji, V. Eutrophication will increase during the 21st century as a result of precipitation changes. *Science* **357**, 405–408 (2017).
15. Wuepper, D., Le Clech, S., Zilberman, D., Mueller, N. & Finger, R. Countries influence the trade-off between crop yields and nitrogen pollution. *Nat. Food* **1**, 713–719 (2020).
16. Ren, C., *et al.* Fertilizer overuse in Chinese smallholders due to lack of fixed inputs. *J. Environ. Manage.* **293**, 112913 (2021).
17. Rosenzweig, C., *et al.* Assessing agricultural risks of climate change in the 21st century in a global gridded crop model intercomparison. *Proc. Natl. Acad. Sci. U. S. A.* **111**, 3268–3273 (2014).
18. Jägermeyr, J., *et al.* Climate impacts on global agriculture emerge earlier in new generation of climate and crop models. *Nat. Food* **2**, 873–885 (2021).
19. Bowles, T.M., *et al.* Addressing agricultural nitrogen losses in a changing climate. *Nat. Sustain.* **1**, 399–408 (2018).
20. Zaveri, E., Russ, J. & Damania, R. Rainfall anomalies are a significant driver of cropland expansion. *Proc. Natl. Acad. Sci. U. S. A.* **117**, 10225–10233 (2020).
21. Wang, X., *et al.* Global irrigation contribution to wheat and maize yield. *Nat. Commun.* **12**, 1235 (2021).
22. Higginbottom, T.P., Adhikari, R., Dimova, R., Redicker, S. & Foster, T. Performance of large-scale irrigation projects in sub-Saharan Africa. *Nat. Sustain.* **4**, 501–508 (2021).
23. Tian, H., *et al.* Global soil nitrous oxide emissions since the preindustrial era estimated by an ensemble of terrestrial biosphere models: Magnitude, attribution, and uncertainty. *Glob. Change Biol.* **25**, 640–659 (2019).
24. Tan, Z., *et al.* Increased extreme rains intensify erosional nitrogen and phosphorus fluxes to the northern Gulf of Mexico in recent decades. *Environ. Res. Lett.* **16**, 54080 (2021).
25. Rousk, K., Sorensen, P.L. & Michelsen, A. What drives biological nitrogen fixation in high arctic tundra: Moisture or temperature? *Ecosphere* **9**, e2117 (2018).

26. Gundale, M.J., Nilsson, M., Bansal, S. & Jäderlund, A. The interactive effects of temperature and light on biological nitrogen fixation in boreal forests. *New Phytol.* **194**, 453–463 (2012).
27. Castellano, M.J., Archontoulis, S.V., Helmers, M.J., Poffenbarger, H.J. & Six, J. Sustainable intensification of agricultural drainage. *Nat. Sustain.* **2**, 914–921 (2019).
28. Wang, J., Klein, K.K., Bjornlund, H., Zhang, L. & Zhang, W. Adoption of improved irrigation scheduling methods in Alberta: An empirical analysis. *Can. Water Resour. J.* **40**, 47–61 (2015).
29. Wang, S., *et al.* Urbanization can benefit agricultural production with large-scale farming in China. *Nat. Food* **2**, 183–191 (2021).
30. Lowder, S.K., Scoet, J. & Singh, S. What do we really know about the number and distribution of farms and family farms worldwide? Background paper for The State of Food and Agriculture 2014. *ESA Working Paper No. 14 – 02. Rome, FAO.* (2014).
31. Wu, Y., *et al.* Policy distortions, farm size, and the overuse of agricultural chemicals in China. *Proc. Natl. Acad. Sci. U. S. A.* **115**, 7010–7015 (2018).
32. Pretty, J., *et al.* Global assessment of agricultural system redesign for sustainable intensification. *Nat. Sustain.* **1**, 441–446 (2018).
33. Gu, B., *et al.* A Credit System to Solve Agricultural Nitrogen Pollution. *The Innovation* **2**, 100079 (2021).
34. Gu, B., Zhang, X., Bai, X., Fu, B. & Chen, D. Four steps to food security for swelling cities. *Nature* **566**, 31–33 (2019).
35. O'Neill, B.C., *et al.* The effect of education on determinants of climate change risks. *Nat. Sustain.* **3**, 520–528 (2020).
36. Roe, S., *et al.* Contribution of the land sector to a 1.5°C world. *Nat. Clim. Chang.* **9**, 817–828 (2019).
37. Mayer, A., Hausfather, Z., Jones, A.D. & Silver, W.L. The potential of agricultural land management to contribute to lower global surface temperatures. *Sci. Adv.* **4**, q932 (2018).
38. Wei, Y., *et al.* Self-preservation strategy for approaching global warming targets in the post-Paris Agreement era. *Nat. Commun.* **11**, 1624 (2020).
39. Hoegh-Guldberg, O., *et al.* The human imperative of stabilizing global climate change at 1.5°C. *Science* **365**, w6974 (2019).
40. Marcacci, G., *et al.* Large-scale versus small-scale agriculture: Disentangling the relative effects of the farming system and semi-natural habitats on birds' habitat preferences in the Ethiopian highlands. *Agric. Ecosyst. Environ.* **289**, 106737 (2020).
41. Li, Y., *et al.* Farmland size increase significantly accelerates road surface rill erosion and nutrient losses in southern subtropics of China. *Soil and Tillage Res.* **204**, 104689 (2020).
42. Li, Y., *et al.* Increase in farm size significantly accelerated stream channel erosion and associated nutrient losses from an intensive agricultural watershed. *Agric. Ecosyst. Environ.* **295**, 106900 (2020).
43. Levins, R.A. & Cochrane, W.W. *The Treadmill Revisited.* University of Wisconsin Press **72**, 550–553 (1996).
44. Ritchie, M. & Ristau, K. *Crisis by Design: A Brief Review of U.S. Farm Policy.* League of Rural Voters Education Project (1986).
45. Ackerman, D., Millet, D.B. & Chen, X. Global Estimates of Inorganic Nitrogen Deposition Across Four Decades. *Glob. Biogeochem. Cycle* **33**, 100–107 (2019).

46. Ortiz-Bobea, A., Ault, T.R., Carrillo, C.M., Chambers, R.G. & Lobell, D.B. Anthropogenic climate change has slowed global agricultural productivity growth. *Nat. Clim. Chang.* **11**, 306–312 (2021).
47. Gu, B., Ju, X., Chang, J., Ge, Y. & Vitousek, P.M. Integrated reactive nitrogen budgets and future trends in China. *Proc. Natl. Acad. Sci. U. S. A.* **112**, 8792–8797 (2015).
48. Zhang, X., *et al.* Ammonia Emissions May Be Substantially Underestimated in China. *Environ. Sci. Technol.* **51**, 12089–12096 (2017).
49. Schlenker, W. & Lobell, D.B. Robust negative impacts of climate change on African agriculture. *Environ. Res. Lett.* **5**, 14010 (2010).
50. Agnolucci, P., *et al.* Impacts of rising temperatures and farm management practices on global yields of 18 crops. *Nat. Food* **1**, 562–571 (2020).

Figures

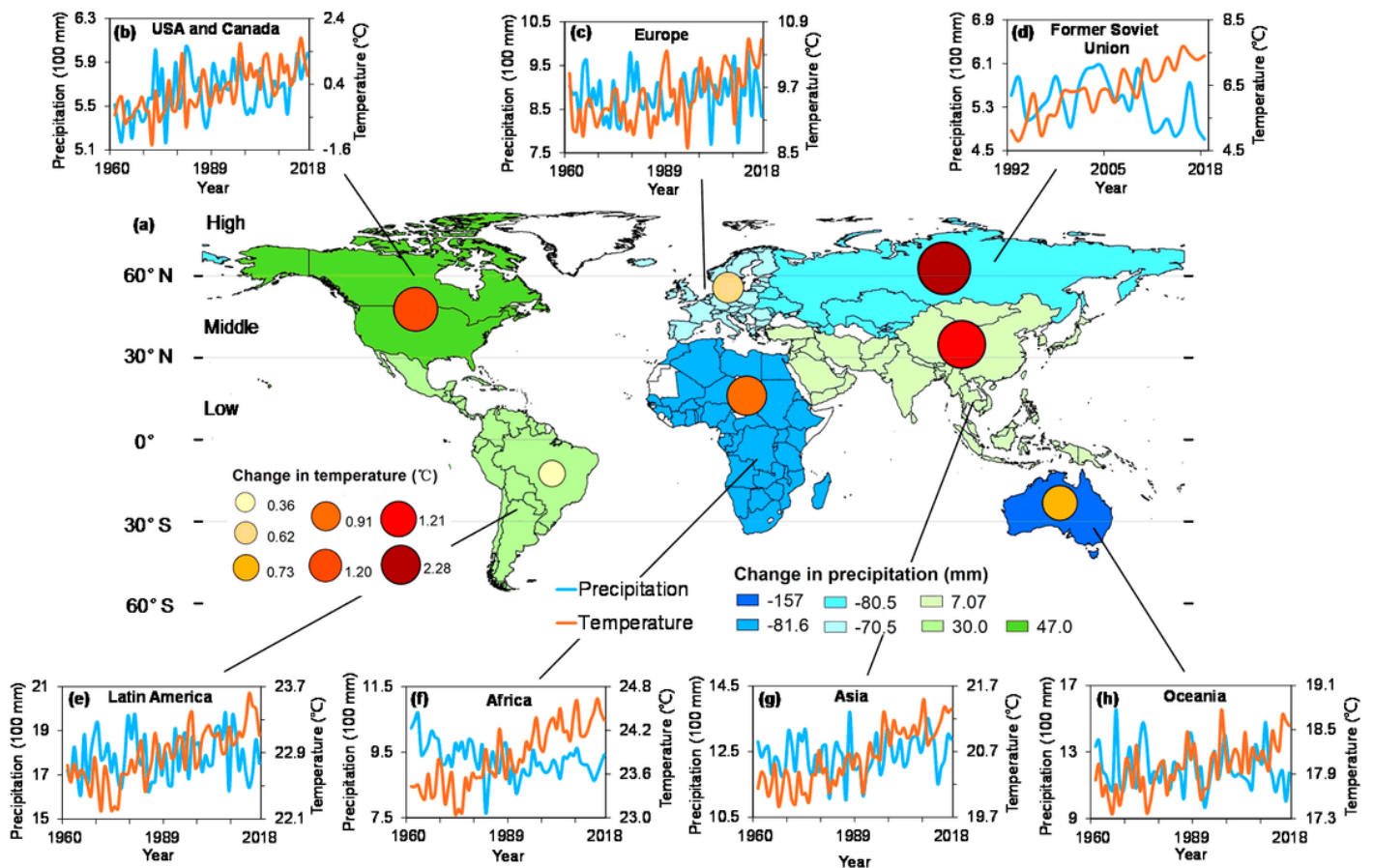


Figure 1

Temperature and precipitation changes across global regions from 1961 to 2018. Panel (a) presents the absolute change of precipitation and temperature between 2018 and 1961. The latitude lines are added in panel (a). Latitudes between 0° and 30°, 30° and 60°, and over 60° are considered low, middle and high latitudes, respectively. The base map is applied without endorsement from GADM data (<https://gadm.org/>). Panel (b)–(i) illustrate the temporal variation of annual precipitation and average temperature by region, which are shown on the primary and secondary axis, respectively.

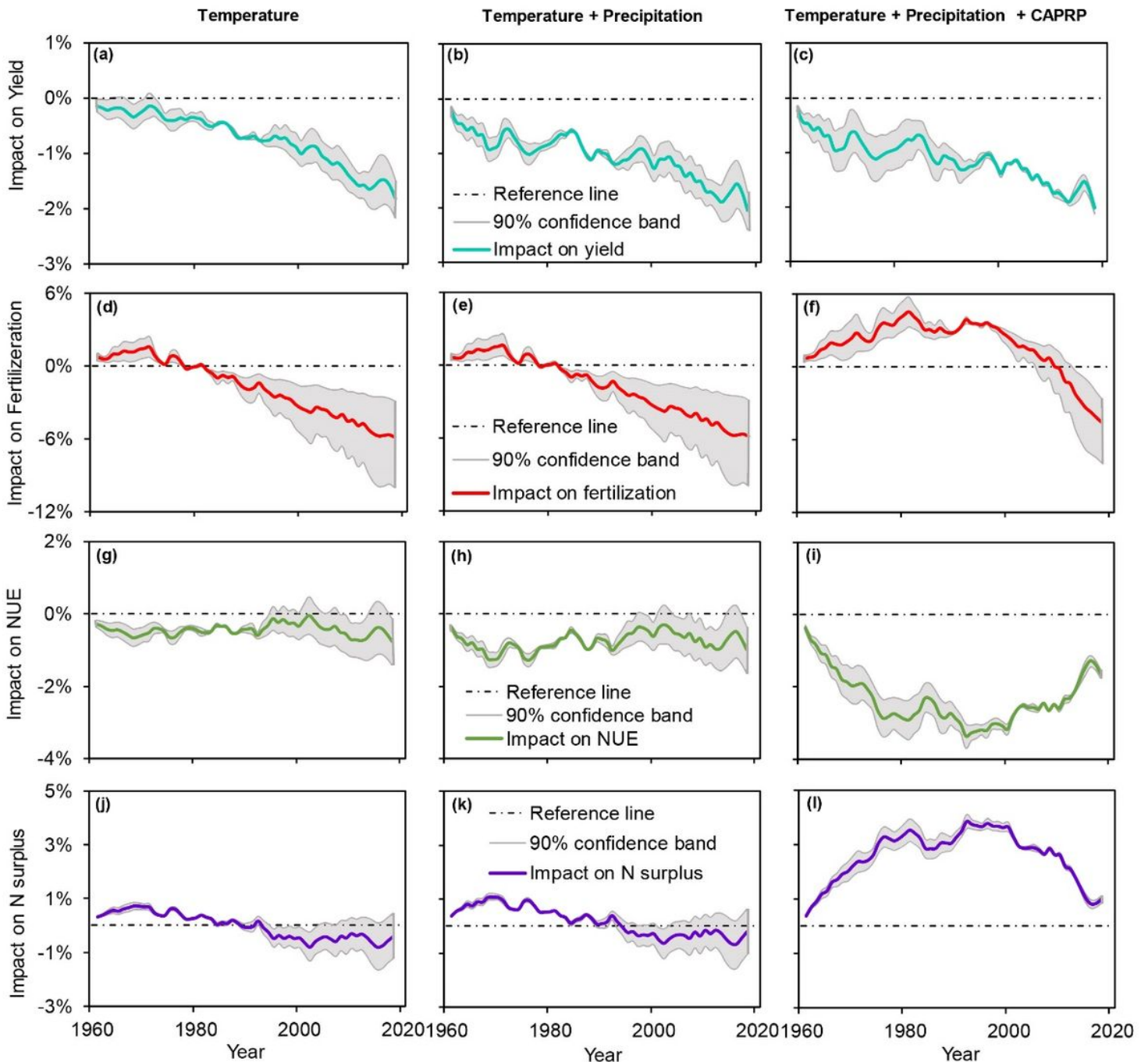


Figure 2

Global impacts of climate and CAPRP changes on yield, fertilization, NUE and N surplus from 1961 to 2018. (a), (d), (g), and (j) present the impacts of temperature changes on yield, fertilization, NUE, and N surplus, respectively. The impacts of climate change are shown in panels (b), (e), (h), and (k). Combined impacts of temperature, precipitation, and CAPRP are depicted in panels (c), (f), (i), and (l). The black dotted line is the reference line equaling to zero, indicating that there is no impact, and the grey cone represents a 90% confidence band based on 5,000 bootstraps estimates. In this figure, the global impacts refer to the relative change (%). It is calculated by the impact divided by the actual observed value subject to climate change in the corresponding year, and the result is carried out in percentage terms. All global means in this figure are weighted and taken as a three-year moving average.

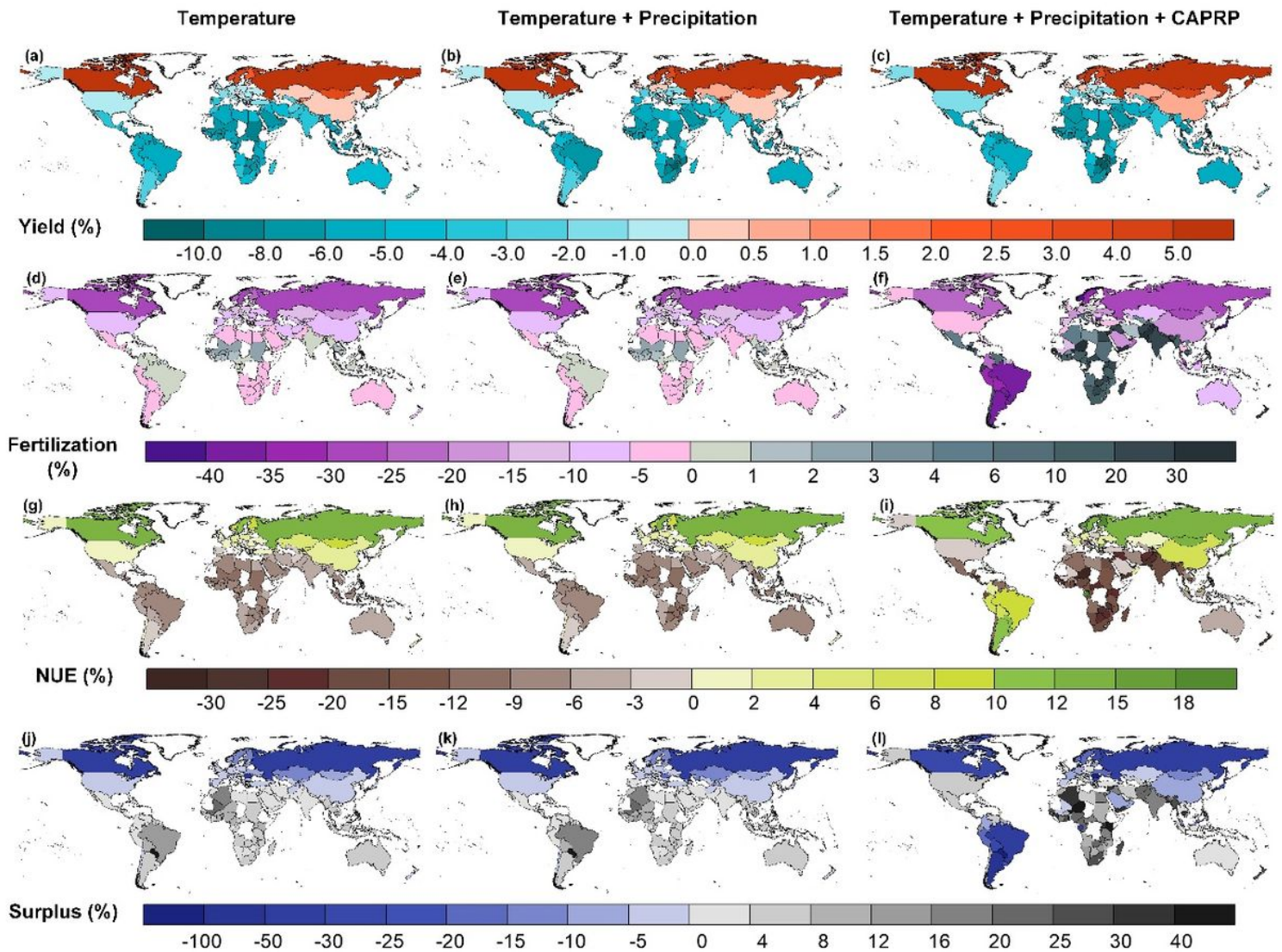


Figure 3

Spatial variability of impact of climate change and CAPRP on yield, fertilization, NUE and N surplus in 2018. (a), (d), (g), and (j) present the spatial impacts of temperature changes on yield, fertilization, NUE, and N surplus, respectively. The spatial impacts of climate change are shown in panels (b), (e), (h), and (k). Combined impacts of temperature, precipitation, and CAPRP are depicted in panels (c), (f), (i), and (l). The impact on each country refers to the relative change (%). It is calculated by the impact divided by the actual observed value subject to climate change in 2018, and the result is carried out in percentage terms. The base map is applied without endorsement from GADM data (<https://gadm.org/>).

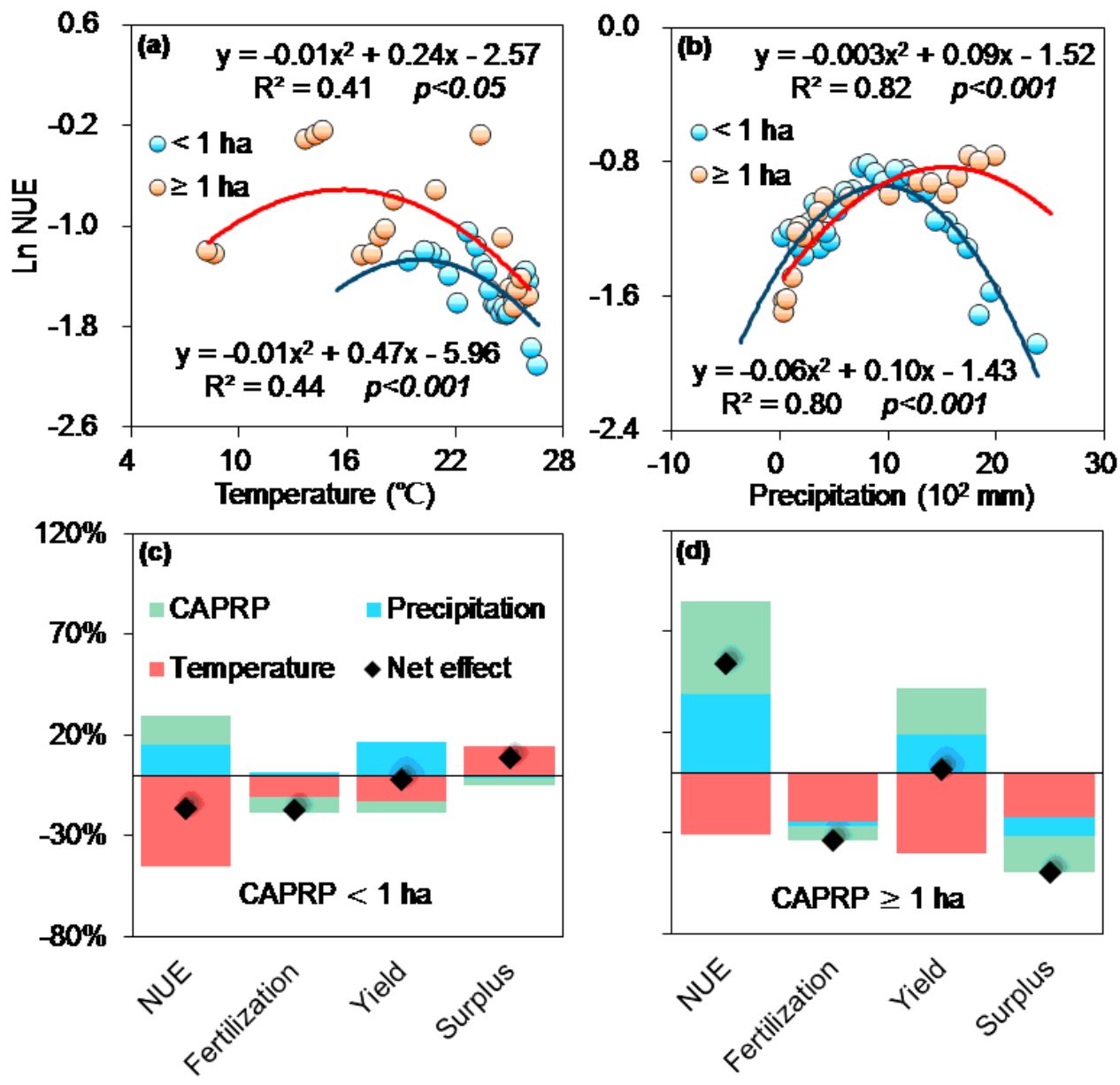


Figure 4

Interaction effect of climate change and CAPRP on cropland N use and loss. Data of panels (a) and (b) depicts the relationship between climate indicators and NUE, which are from Latin America and Africa, respectively. Each data point represents an average value of the log-transformed NUE within a certain temperature and precipitation group (about 50 groups totally in each panel), respectively, which can be found in SI Table S8. Panel (c) and (d) show the relative effects of climate change and CAPRP on NUE, fertilization, yield and N surplus changes among small and large CAPRP groups (< 1 ha and ≥ 1 ha, respectively). The effects were derived from the ratio of the standardization coefficient of each explanatory variable to the standard deviation of the explained variable according to Eq. (5) covering all sample countries from 1961 to 2018. The effect from temperature depicted in panel (c) were summed the effects from itself and its quadratic items in each CAPRP group. The precipitation effect is estimated in the same way.

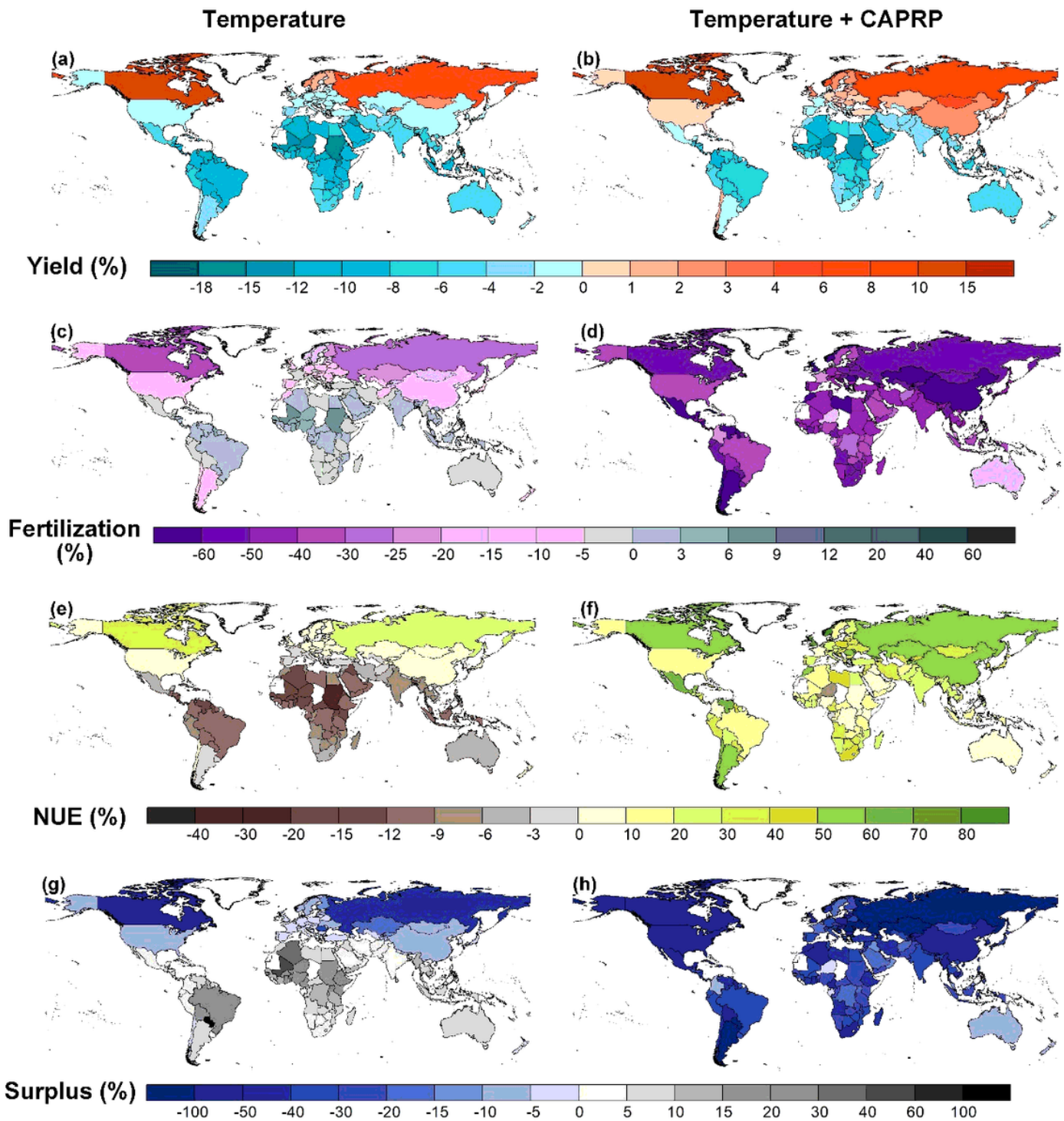


Figure 5

Yield, fertilization, NUE and N surplus changes in 2100 under the optimal SSP1 scenario (SSP1). Value changes refer to the relative change (%) in this figure. It is calculated by the value difference simulated between 2018 and 2100 under the SSP1 scenario divided by the actual observed value subject to climate change in 2018 and the result is carried out in percentage terms. The left panel shows changes under the SSP1 scenario only considering the temperature. The right panel represents changes further considering the role of CAPRP. The base map is applied without endorsement from GADM data (<https://gadm.org/>).

Supplementary Files

This is a list of supplementary files associated with this preprint. Click to download.

- [SupplementaryMaterials.docx](#)
- [ExtendedDataFiguresandTables.docx](#)